LOCAL VOLATILITY MODEL APPLIED TO BIST30 EUROPEAN WARRANTS:PRICING AND HEDGING

A THESIS SUBMITTED TO
THE GRADUATE SCHOOL OF APPLIED MATHEMATICS
OF
MIDDLE EAST TECHNICAL UNIVERSITY

BY

ZEKİYE SILA KİRAZOĞLU

IN PARTIAL FULFILLMENT OF THE REQUIREMENTS
FOR
THE DEGREE OF MASTER OF SCIENCE
IN
FINANCIAL MATHEMATICS

SEPTEMBER 2016

Approval of the thesis:

LOCAL VOLATILITY MODEL APPLIED TO BIST30 EUROPEAN WARRANTS:PRICING AND HEDGING

submitted by **ZEKİYE SILA KİRAZOĞLU** in partial fulfillment of the requirements for the degree of **Master of Science in Department of Financial Mathematics, Middle East Technical University** by,

Prof. Dr. Bülent Karasözen
Director, Graduate School of **Applied Mathematics** _____

Assoc. Prof. Dr. Yeliz Yolcu Okur
Head of Department, **Financial Mathematics** _____

Assoc. Prof. Dr. Ali Devin Sezer
Supervisor, **Financial Mathematics, METU** _____

Examining Committee Members:

Prof. Dr. Fatih Tank
Department of Insurance and Actuarial Sciences, Ankara Üniversitesi _____

Assoc. Prof. Dr. Ali Devin Sezer
Financial Mathematics, METU _____

Prof. Dr. Gerhard Wilhelm Weber
Financial Mathematics, METU _____

Date: _____

I hereby declare that all information in this document has been obtained and presented in accordance with academic rules and ethical conduct. I also declare that, as required by these rules and conduct, I have fully cited and referenced all material and results that are not original to this work.

Name, Last Name: ZEKİYE SILA KİRAZOĞLU

Signature :

ABSTRACT

LOCAL VOLATILITY MODEL APPLIED TO BIST30 EUROPEAN WARRANTS:PRICING AND HEDGING

KİRAZOĞLU, Zekiye Sıla
M.S., Department of Financial Mathematics
Supervisor : Assoc. Prof. Dr. Ali Devin Sezer

September 2016, 43 pages

One of the basic observations on pricing options is that the assumption of constant volatility does not agree with data and market price data gives a volatility smile that depends on maturities and strike prices. The first model that developed to be compatible with this observation is the local volatility model. The purpose of this work is to study the performance of the local volatility model on BIST30 warrants and compare it to the standard Black Scholes model. To estimate the local volatility model from data two approaches are used: 1) we estimate the local volatility directly from the underlying data (in this approach we make two assumptions: a) the local volatility depends only on the price of the underlying b) the local volatility is a piecewise linear function) 2) first a Heston model is fit to option prices and we use Dupire's formula to derive the implied local volatiliy model.

Keywords : The Local Volatility Model, BIST30, warrants, pricing, hedging

ÖZ

BIST30 ALIM SATIM VARANTLARINA YEREL VOLATİLİTE MODELLERİNİN UYGULANMASI

KİRAZOĞLU, Zekiye Sıla
Yüksek Lisans, Finansal Matematik Bölümü
Tez Yöneticisi : Doç. Dr. Ali Devin Sezer

Eylül 2016, 43 sayfa

Opsiyon fiyatlamada temel gözlemlerden biri sabit volatilite varsayımının verilerle uyuşmadığı ve market fiyat verilerinin vadeye ve kullanım değerine bağlı bir "volatilite eğrisi" (volatility smile) verdiğidir. Bu gözlemle uyum kurmak için geliştirilen modellerden ilki "yerel volatilite" (local volatility) modelleridir. Bu çalışmanın amacı Yerel volatite modellerinin BIST30 üzerine yazılmış alım satım varantlarının fiyatlama ve üretme (replication) performansını çalışmak ve Black Scholes modeliyle karşılaştırmaktır. Veriden yerel volatilite modeli çıkarımı için iki yöntem izlenmiştir 1) dayanak varlığın geçmiş fiyat hareketlerinden çıkarım (bu yöntem için iki varsayım yapılmıştır a) yerel volatilite sadece dayanak varlığın değerine bağlı kabul edilmiştir b) yerel volatilite fonksiyonu yerel olarak lineer kabul edilmiştir) 2) ilk olarak opsiyon fiyatlarından Heston modeli çıkarımı yapılmış ve Dupire formülü kullanılarak Heston parametrelerinin karşılık geldiği yerel volatilite fonksiyonu çıkarımı yapılmıştır.

Anahtar Kelimeler : Yerel Volatilite Modeli,BIST30,varant, fiyatlama, üretme

To My Family

ACKNOWLEDGMENTS

I would like to express my gratitude to my thesis advisor Assoc. Prof . Dr . Ali Devin Sezer for his endless help and patience. I could not finish this thesis without his encouragement and guidance.

I would like to thank Emre Ünver working in İş Yatırım for helping me to find my thesis subject and provide some resources and information.

I would like to thank my friends and my family for their support, patience and motivation.

I would like to thank the examining committee members, Assoc. Prof. Dr. Ali Devin Sezer, Prof. Dr. Gerhard-Wilhelm Weber and Prof. Dr. Fatih Tank for their suggestions, corrections and comments.

TABLE OF CONTENTS

LIST OF FIGURES

LIST OF TABLES

LIST OF ABBREVIATIONS

S_t	The Stock Price at time t
x_t	The Log Stock Price at time t
r_t	The Instantenous Risk-Free Rate
d_t	Dividend Yield
W	The Brownian Motion
λ	The Market Price of Volatility Risk
κ	The Mean Reversion Speed
θ	The Mean Reversion Level
σ	The Volatility of the Variance
v_0	Initial Variance
ρ	The Correlation between the two Brownian motions

CHAPTER 1

Introduction

The standard classical model in option pricing is the Black Scholes (BS) model first given in [1], see also [15]. Black Scholes model is the benchmark model also in finance practice: the reason for its dominance is the simple explicit formulas it gives for pricing and hedging. The simplicity of these come from the model assumptions, namely constant interest rate and volatility. One indication of the prominence of this model in practice is the term "implied volatility:" by definition the implied volatility of a given European option is the volatility value in the Black Scholes model under which the model gives exactly the price observed in the market. If the BS model were a consistent model for option prices all options on the same underlying stock would have the same implied volatility even if they have different strikes or different maturities. Unfortunately such consistency doesn't exist in real markets and the implied volatilities of options written on the same underlying do change with strikes and maturities (these collection of implied volatilities is called a volatility smile) [7]. What is the simplest extension of the BS model to account for the volatility smile? Perhaps the simplest extension would be to replace the constant volatility with a volatility which is allowed to depend deterministically on time and the price of the underlying; this is the local volatility model and its first analyses began with [5, 4]. In the paragraphs below we review this model.

The Local Volatility model is an extension of the standard Black Scholes model where the constant volatility $\sigma \in \mathbb{R}_+$ is replaced with a function $\sigma : (s,t) \to \mathbb{R}_+$; thus the volatility is made a deterministic function of the current asset price and time. There are a number of studies in the literature which explain why this model is called a local volatility model and its further motivations, see, e.g, [10, 7]. The main practical motivation for local volatility models consists of two points

1. There is only one source of randomness, i.e., the Brownian motion driving the stock price,and hence the model leads to a complete market and it allows a perfect hedge of European derivatives in continuous time with a portfolio consisting of only the underlying stock and bonds.

2. Given a perfect and smooth implied volatility surface of standard European options (i.e., a volatility surface in which all maturities and strikes are represented) there is a unique local volatility model which matches exactly the given surface; hence, at least in theory, local volatility models can perfectly match given Euro-

pean option prices on any given day. This relation is known as Dupire's formula, and is reviewed in the next chapter.

The aim of this thesis is to study the applicability and performance of the Local Volatility model to standard call options written on the BIST30 index [1], which is one of the most popular stock indices that tracks 30 of the most traded stocks in the Borsa İstanbul and compare its performance to the standard Black-Scholes model.

Chapter 2 is a review of the Local Volatility model: its definition, the derivation of the partial differential equation (PDE) satisfied by European option prices under the local volatility modela and a derivation of Dupire's formula. This chapter mainly follows [7, 5, 16]. Chapters 3 and 4 present our main work and results. As stated, our goal is to fit the local volatility model to warrants written on the BIST30 index which are currently traded in Borsa Istanbul and study the hedging and pricing performance of the model. For this work, we use the publicly available daily prices. Therefore, the delta hedging algorithm implied by the local volatility model is also applied daily. This discretization and model error will lead to an accumulated hedging error which will be updated each time the hedging portfolio is updated; the details of this computation is given in section 3.2.3. This hedging error, normalized by the price of the option will be our main performance criterion.

In fitting the local volatility model to data we try two approaches: in Chapter 3 we directly use the values of the BIST30 index to estimate the local volatility function; we refer to this as "fitting using historical data." To simplify our task we make the following assumptions

1. the local volatility function depends only on the price of the underlying
2. the local volatility function is piecewise linear in the $\log$ of the underlying price.

Further details, of the fitting process, starting from these assumptions are given in Chapter 3. In Chapter 4 we use the approach suggested in [7]: first fit the Heston model to the derivative prices and use Dupire's formula to get a local volatility surface. The fits used in this thesis come from [14]. In computing the local volatility function we use an approximation developed by Gatheral. The derivation of this approximation, following [16] is also given in Chapter 4.

In addition to the model fits, both chapters study the hedging performance of the fitted models. For our hedge study, we look at two periods over which the hedging algorithm is run: 15.01.2016- 05.02.2016 and 01.03.2016- 31.03.2016. All of the hedged warrants are call type. For the January period we use strike price- 90 and two maturities: 29.02.2016 and 29.04.2016. For the March period we use strike price- 95 and two maturities: 29.04.2016- 30.06.2016. All of the warrants hedged in these chapters were traded (and had market prices) during the periods over which we run the hedging algorithm. This leads to a further choice in the implementation of the hedging algorithm

[1] This is one of the main indices tracking asset prices observed in Borsa Istanbul, for more info on it see `http://www.borsaistanbul.com/endeksler`.

when the fit is done from historical data as in Chapter 3: in the hedging one can either use the model prices or the market prices. In Chapter 3 both of these possibilities are tried. Our main finding on this choice is that the market prices lead to a much better hedge compared to the model prices. All hedges are also repeated with the Black scholes model and the results are compared with those given by the local volatility model. A detailed comparison is given in Chapters 3 and 4; based on the results of these chapters our overall impression is that the local volatility models do not hedge significantly better than simple Black Scholes, and their performances are similar.

In all of the computations the interest rate is taken to be constant and is estimated from the average of the benchmark interest rate [2] over a single month preceding the hedge period.

Conclusion comments on future work.

[2] see, e.g, `http://www.bloomberght.com/tahvil/gosterge-faiz`

CHAPTER 2

Local Volatility Models

This chapter gives a definition of local volatility models and Dupire's formula [5, 7], which connects prices to the local volatility functions.

2.1 The Model

Consider the following general model often used to model an asset price:

$$dS_t = (\mu_t - d_t)S_t dt + \sigma_t S_t dW_t, \tag{2.1}$$

where μ_t is the average growth rate of the stock and d_t is the dividend yield assumed to be zero in this study, W_t is a Brownian motion and the σ_t is the volatility at time t. In addition to the stock price modeled by Equation 2.1 the market is also equipped with an instantenous interest rate r_t. In the Black-Scholes model, $\sigma_t = \sigma$ and $r_t = r$ are assumed to be constant; in local volatility models the constany assumption on σ is modified to

$$\sigma_t = \sigma(t, S_t)$$

where $\sigma(\cdot, \cdot)$ is a deterministic function of time and the current stock price. For the purposes of this thesis we will assume $d_t = 0$; in pricing options in an arbitrage free framework the average growth rate μ_t plays no role, and we will assume it to be a cosntant μ. Thus, we arrive at the following basic local volatility model for the price movement of a stock.

$$dS_t = \mu S_t d_t + \sigma(t, S_t)S_t dW_t. \tag{2.2}$$

The existence uniqueness theory asssociated with this stochastic differential equation (SDE) is classical, see [11, Chapter 5], a simple sufficient condition for the existence and uniqueness of the solution to Equation 2.3 is the Lipschitz continuity of $\sigma(\cdot, \cdot)$ in the x variable. The piecewise linear models of local volatility we use in this thesis does satisfy this condition.

The solution of S_t of Equation 2.3 gives us the price of a risky asset in our market. The constant riskless rate r gives the second component of this market, the bond price:

$$S_t^{(0)} = e^{rt}.$$

Pricing European derivatives under the model given above is classical and one can find a thorough exposition in it in [13]. Let us very briefly indicate the elements of this theory. Let us denote $(\Omega, \mathscr{F}, P)$ the probability space on which is constructed the SDE Equation 2.3 and let $\mathscr{F}_t$ be the filtration generated by W. One constructs a new martingale measure P^* on $(\Omega, \mathscr{F})$ under which the process

$$W_t^* = \int_0^t \frac{\mu - r}{\sigma(s, S_s)} ds + W_t$$

is a Brownian motion. The existence of the measure P^* is given by Girsanov's theorem, for the details we refer the reader to [13]. Under P^* the dynamics Equation 2.3 become

$$dS_t = rS_t d_t + \sigma(t, S_t) S_t dW_t^*. \tag{2.3}$$

For the rest of this thesis these risk neutral dynamics will be assumed for the risky asset price.

Consider a European option with payoff $g(S_T)$ where the function $g : \mathbb{R} \to \mathbb{R}_+$ represents the payoff structure. Under basic intergrability assumptions on $g(S_T)$, a well known fact in mathematical finance [13] is that the no arbitrage price of this option at time $t < T$ equals

$$V(t, S_t) = e^{-r(T-t)} \mathbb{E}^*[g(S_T)|\mathscr{F}_t].$$

A well known method to compute the function V is to derive a PDE which it satisfies and (perhaps numerically) solve this PDE. This derivation is well known; we review it in the next section within the context of the local volatility model. The derivation rests on the construction of an arbitrage free portfolio containing one unit of the option to be priced and Δ units of the underlying asset. The Δ value can then be used to actually replicate the payoff of the option. When such a replicating portfolio exists for all contingent claims, we say that the market is complete; thus the argument of the next section also implies the completeness of the market (at least for European options).

2.2 Derivation of the Local Volatility PDE

In the Black Scholes model, to derive the PDE satisfied by the price of a European option one begins by a portfolio consisting of Δ units of the underlying asset and 1 unit of the option to be hedged; then the coefficient Δ is chosen so that the portfolio value becomes deterministic. This procedure produces two outcomes: 1) the PDE satisfied by the price V and 2) the Δ amount which can be used when replicating the option. It is well known that the Δ turns out to be $V_x(t, S_t)$. The details of this derivation is already given in [13] and many standard textbooks on mathematical finance. For readers convenience we overview below its steps in the context of the local volatilty model. All of the calculation below are done under the risk neutral measure; to ease notation we will denote the risk neutral brownian motion by W.

We begin with a portfolio $(1, \Delta)$ consisting of one unit of the option to be priced and Δ unit of the underlying stock. We want to choose Δ so that the portfolio value becomes

a deterministic function of time. The value Π of the portfolio is

$$\Pi_t = V(t, S_t) + \Delta_t S_t$$

We will construct the portfolio to be selffinancing so that $e^{-rt}\Pi_t$ will be a martingale under P^*. The change in the portfolio is

$$d\Pi_t = dV(t, S_t) + d(\Delta t S_t). \tag{2.4}$$

Application of Ito's formula gives

$$V = V_0 + \int_0^t \frac{\partial V}{\partial s} ds + \int_0^t \frac{\partial V}{\partial S} dS + \frac{1}{2} \int_0^t \frac{\partial^2}{\partial S^2} d \left\langle S \right\rangle_s . \tag{2.5}$$

Using the fact that $d \left\langle S \right\rangle_s = \sigma(t, S_t)^2 S(t, S_t)^2 dt$ and $dS = rS_t dt + \sigma S_t dW_t$ from Equation 2.1 and differentiating Equation 2.5 with respect to t,

$$dV = \frac{\partial V}{\partial t} dt + \mu S \frac{\partial V}{\partial S} dt + \frac{1}{2} \sigma^2 S^2 \frac{\partial^2}{\partial S^2} dt + \sigma S \frac{\partial V}{\partial S} dW \tag{2.6}$$

To find ΔS we can multiply Equation 2.1 with Δ,

$$\Delta dS = \Delta \mu S dt + \Delta \sigma S dW \tag{2.7}$$

If we combine Equation 2.5 and Equation 2.7 we get,

$$\begin{aligned} d\Pi = \left(\frac{\partial V}{\partial t} + rS \frac{\partial V}{\partial S} + \frac{1}{2} \sigma^2 S^2 \frac{\partial^2 V}{\partial S^2} + \Delta \mu S \right) dt \\ + \left(\sigma S \frac{\partial V}{\partial S} + \Delta \sigma S \right) dW \end{aligned} \tag{2.8}$$

Since we have a riskless portfolio the coefficient of dW must be equal to zero, in other words,

$$\left(\sigma S \frac{\partial V}{\partial S} + \Delta \sigma S \right) = 0$$

which means

$$\Delta = -\frac{\partial V}{\partial S}. \tag{2.9}$$

Here, Δ is called hedge parameter. Subsituting Δ in Equation 2.8 and equating the coefficient of dW zero give

$$d\Pi = \left(\frac{\partial V}{\partial t} + \frac{1}{2} \sigma^2 S^2 \frac{\partial^2 V}{\partial S^2} \right) dt. \tag{2.10}$$

Since the portfolio is riskless and the market is arbitrage free, the payoff portfolio must be equal to the risk-free rate, r. That is, $d\Pi = r\Pi dt$. Therefore, Equation 2.10 becomes

$$d\Pi = r(V + \Delta S) dt \tag{2.11}$$

This and Equation 2.10 give

$$\frac{\partial V}{\partial t} + \frac{1}{2}\sigma^2 S^2 \frac{\partial^2 V}{\partial S^2} = r(V + \Delta S),$$

Substituting to this the value of Δ found in Equation 2.9 we get the PDE we seek:

$$-rV + \frac{\partial V}{\partial t} + rS\frac{\partial V}{\partial S} + \frac{1}{2}\sigma(t,x)^2 S^2 \frac{\partial^2 V}{\partial S^2} = 0. \tag{2.12}$$

This is a linear parabolic PDE. The payoff g of the option is used to supply a boundary condition to Equation 2.12:

$$V(T,x) = g(x).$$

The equation Equation 2.12 is a classical equation; remember our Lipschitz continuity assumption on σ. This assumption suffices to get smooth solutions to Equation 2.12, when g has enough intergrability [6]. In the next section we will solve this PDE numerically to compute prices of call options on BIST30.

2.3 Dupire's Formula

Perhaps the most important formula connected to the local volatility model Equation 2.3 is Dupire's formula, which is the name of the following relation:

$$\frac{\partial C}{\partial \tau}(\tau, K) = \frac{K^2\sigma^2(\tau,K)}{2}\frac{\partial^2 C}{\partial K^2}(\tau, K)$$

where $C(\tau, K)$ is the price of the call option with maturity τ and strike K. A derivation of Dupire's Formula is given in Appendix 2.4. The significance of this formula is that it allows us to compute the local volatility from the price function C thus:

$$\sigma^2(K,T,S_0) = 2\frac{\frac{\partial C}{\partial T}}{K^2\frac{\partial^2 C}{\partial K^2}} \tag{2.13}$$

See the next section for a derivation of this formula. In theory, the right hand side of Equation 2.13 can be computed from known European option prices. We say "in theory" because, the computation of the derivatives of C requires that we have a complete set of European option prices for all strikes and expirations, which is not available in real life. An approach suggested by [7] to overcome this difficulty is as follows: one first fits another volatility model, such as the Heston model, to the known prices, and then one uses Equation 2.13 to get the implied local volatility model. We will use this approach in Chapter 4.

2.4 Derivation of Dupire's Formula

In this section we give a derivation of the Dupire's equation step by step. The outline of the following computation is given as an exercise in [13].

Step 1: Let us begin with showing Equation 2.1 has a unique solution such that $S_0 = x$ for every $x \in R$:

From Ito formula, we have;

$$S_t = S_0 + \int_0^t \mu(s)S_s ds + \int_0^t \sigma(s, S_s)S_s dW_s + \frac{1}{2}\int_0^t S_s^2\sigma^2(s, S_s)ds \tag{2.14}$$

Therefore, if we write S_0=x for all x in Equation 2.14, we obtain unique S_t for each x that we equalize to S_0.

Step 2: Secondly, we can show that the solution S_t have an exponential form. That is;

Let $X_t = \log(S_t)$;i.e. $S_t = \exp(X_t)$.Then if we apply Ito's Formula on X_t, we get;

$$X_t = X_0 + \int_0^t \mu(s)S_s\frac{1}{S_s}ds + \int_0^t \sigma(S_s, s)S_s\frac{1}{S_s}dW_s + \frac{1}{2}\int_0^t (-\frac{1}{S_s^2})S_s^2\sigma^2(S_s, s)ds \tag{2.15}$$

After some arrangements in Equation 2.15, we obtain;

$$X_t = X_0 + \int_0^t \mu(s)ds + \int_0^t \sigma(S_s, s)dW_s - \frac{1}{2}\int_0^t \sigma^2(S_s, s)ds \tag{2.16}$$

If we take an exponential of both sides of Equation 2.16;

$$A = e^{X_t} = S_t = e^{X_0}e^{\int_0^t \mu(s)ds + \int_0^t \sigma(S_s,s)dW_s - \frac{1}{2}\int_0^t \sigma^2(S_s,s)ds} \tag{2.17}$$

Hence, we get;

$$S_t = S_0 \exp[\int_0^t \mu(s)ds + \int_0^t \sigma(S_s, s)dW_s - \frac{1}{2}\int_0^t \sigma^2(S_s, s)ds] \tag{2.18}$$

Step 3: Now, we should prove that the natural filtration of the process $(S_t)_{t\geq 0}$ is equal to F(which is the notation of the natural filtration of $(B_t)_{t\geq 0}$). Let $Z_t = \log(S_t)$, then

$$Z_t = Z_0 + \int_0^t \mu(s)ds + \int_0^t \sigma(s, S_s)dW_s - \frac{1}{2}\int_0^t \sigma^2(S_s, s)ds \tag{2.19}$$

We know our first assumption that $S_t = e^{Z_t}$, so $S_s = e^{Z_s}$. Then if we plug S_s in the Equation 2.19, we obtain:

$$Z_t = Z_0 + \int_0^t \mu s ds + \int_0^t \sigma(s, e^{Z_s})dW_s - \frac{1}{2}\int_0^t \sigma^2(s, e^{Z_s})ds \tag{2.20}$$

If we divide both sides by Z_t and then integrate from 0 to t, we get:

$$\int_0^t \frac{1}{\sigma(s,e^{Z_s})}dZ_s = \int_0^t \frac{Z_0}{\sigma(s,e^{Z_s})}ds + \int_0^t \frac{\mu(s)}{\sigma(s,e^{Z_s})}ds + W_t - \frac{1}{2}\int_0^t \sigma(s,e^{Z_s})ds \tag{2.21}$$

Finally, if we leave W_t alone in Equation 2.21;

$$W_t = \int_0^t \frac{1}{\sigma(s,e^{Z_s})}dZ_s - \int_0^t \frac{Z_0}{\sigma(s,e^{Z_s})}ds - \int_0^t \frac{\mu(s)}{\sigma(s,e^{Z_s})}ds + \frac{1}{2}\int_0^t \sigma(s,e^{Z_s})ds \tag{2.22}$$

OR if we write S_s instead of e^{Z_s} in Equation 2.22;

$$W_t = \int_0^t \frac{1}{\sigma(s,S_s)}dS_s - \int_0^t \frac{\log S_0}{\sigma(s,S_s)} - \int_0^t \frac{\mu(s)}{\sigma(s,S_s)}ds + \frac{1}{2}\int_0^t \sigma(s,S_s)ds \tag{2.23}$$

which is equal to;

$$W_t = \int_0^t \frac{1}{\sigma(s,S_s)}dS_s - \int_0^t [\frac{\log(S_0)+\mu(s)}{\sigma(s,S_s)} - \frac{\sigma(s,S_s)}{2}]ds \tag{2.24}$$

All of these means that if we know process $(S_t)_{t\geq 0}$,then we can find W_t in terms of S_t.

Step 4: Let L be martingale defined by $L_t = \exp\left(-\int_0^t \Theta_u dW_u - \frac{1}{2}\int_0^t \Theta_u^2 du\right)$,with $\Theta_t = \frac{\mu(t)}{\sigma(t,S_t)}$. Fix the horizon $\tilde{\tau}$ of the model $(0 < \tilde{\tau} < +\infty)$ and let $P^\star$ be the probability given by $\frac{dP^\star}{dP} = L_{\tilde{\tau}}$. Given $\tau \in [0,\tilde{\tau}]$, let $C(\tau,K)$ be the price of a call option with maturity τ and strike price K.

(a) We should prove that, for $(t,x) \in R^+$, $\sigma(t,x) \leq M$.In adddition to this, we should deduce that, for $0 \leq t \leq \tilde{\tau}$ and $p \geq 1$, $E^\star(S_t^p) \leq S_0^p exp\left(\frac{p^2-p}{2}M^2 t\right)$:

To reach a solution, first we should take $f(S_t) = S_t^p$ then we should apply the Ito's Formula on $f(S_t)$;

$$f(S_t) = f(S_0) + \int_0^t f'(S_s)dS_s + \frac{1}{2}\int_0^t f''(S_s)d < S >_s \tag{2.25}$$

OR equivalently;

$$S_t^p = S_0^p + \int_0^t pS_s^{p-1} S_s \sigma(s, S_s) dB_s + \int_0^t pS_s^{p-1} S_s \mu(s) ds + \frac{1}{2} \int_0^t p(p-1) S_s^{p-2} S_s^2 \sigma^2(s, S_s) ds \tag{2.26}$$

If we take expectation of the both sides of Equation 2.26;

$$E^\star[S_t^p] = E^\star[S_0^p] + pE^\star[\int_0^t S_s^p \mu(s) ds] + \frac{p(p-1)}{2} E^\star[\int_0^t S_s^p \sigma^2(s, S_s) ds] \tag{2.27}$$

Since expectaiton of Brownian Motion is zero and drift term is given by zero, after doing this elimination in Equation 2.27 we have;

$$E^\star[S_t^p] = E^\star[S_0^p] + \frac{p(p-1)}{2} E^\star[\int_0^t S_s^p \sigma^2(s, S_s) ds] \tag{2.28}$$

Since $\sigma^2 \leq M^2$, we have $E^\star[S_t^p] \leq E^\star[S_0^p] + \frac{p(p-1)}{2} E^\star[\int_0^t S_s^p M^2 ds]$ which is equivalently;

$$E^\star[S_t^p] \leq E^\star[S_0^p] + \frac{p(p-1)}{2} M^2 E^\star[\int_0^t S_s^p ds] \tag{2.29}$$

Now, to reach the desired conclusion we should use Gronwall's Inequality which says;

If we have an equality such that $\psi(t) = \psi(0) + c\int_0^t \psi(s) ds$ where c is a constant, then by taking derivative we have $\psi'(t) = c\psi(t)$ and we know that the solution of this equality $\psi(t) = \psi(0)e^{ct}$. If we use inequality instead of equality, we have $\psi(t) \leq \psi(0)e^{ct}$.If we turn back our inequality, we see that here the constant $c = \frac{p^2-p}{2} M^2$ and we conclude that;

$$E^\star[S_t^p] \leq S_0^p e^{\frac{p^2-p}{2} M^2 t} \tag{2.30}$$

(b) The explanation of the equality $C(\tau, K) = E^\star[(S_\tau - K)_+]$ for $\tau \in [0, \tilde{\tau}]$ is;
Since $E^\star$ is taken under $P^\star$ that is the risk neutral probablity measure, the equality above makes sense in term of that pricing a call option in risk neutral expectation, which gives us an oppurtunity that we can act freely in risk neurtral environment as a risk neutral investor.

(c) To show that, for $K \geq 0$, $\tau \to C(\tau, K)$ is nondecreasing on $[0, \tilde{\tau}]$ we use the martingale property of S under $P^\star$. Moreover, we prove that $(\tau, K) \to C(\tau, K)$ is continuous on $[0, \tilde{\tau}] \times R^+$:

Let f be a convex function and M be a martingale, then $E^\star[f(M_t)|F_s] \geq f[E^\star[M_t|F_s]]]$. Here, since $E^\star[M_t|F_s]] = M_s$ we have $E^\star[f(M_t)|F_s] \geq f(M_s)$ which means that $t \to f(M_t)$ is a submartingale. [13]
Let $\tau \to (S_\tau - K)_+ = f(M_\tau) = C(\tau, K)$, then from the expectation rules we know that $E^\star[E^\star[X|G]] = E^\star[X]$ where G is the probability measure. Therefore; $E^\star[E^\star[f(M_t)|F_s]] \geq E^\star[f(M_s)]$. In other words if $t \geq s$ then $E^\star[f(M_t)] \geq E^\star[f(M_s)]$ which means that $\tau \to C(\tau, K)$ is non-decreasing on $\tau \in [0, \tilde{\tau}]$

Now, to prove continuity, let $Y_n = (S_{\tau_n} - K_n)_+$ so that $Y = (S_\tau - K)_+$ when $n \to \infty$. Fix $\omega \in \Omega$. If $Y_n(\omega) \to Y(\omega)$ for $\omega \in \Omega$, then, using Dominated Convergence Theorem we need to show that $E^\star[Y_n] \to E^\star[Y]$, i.e. we need to put the limit inside of $E^\star$.To do this, we only need to show that $|Y_n| \leq Z$ for $Z \in R$.Thus, for a fixed $\omega \in \Omega$.

$$|Y_n| = (S_{\tau_n} - K_n)_+ \leq |S_{\tau_n}(w)|^+ \leq \max_{t \in \tilde{\tau}} |S_t(w)| \tag{2.31}$$

Therefore, $E^\star[Y_n] \to E^[Y]$. This means that $C(\tau_n, K_n) \to C(\tau, K)$. This proves that $(\tau, K) \to C(\tau, K)$ is continuous on $[0, \tilde{\tau}] \times R^+$.

(d) Now, we need to make a connection with the E^* and the call price C:

First we need to check that $(S-K)_+^2 = 2\int_K^\infty (S-u)^+ du$. Now,
let $S \leq K$, then $2\int_K^S (S-u)^+ du + 2\int_S^\infty (S-u)^+ du = 2\int_K^S (S-u)^+ du$ since $2\int_S^\infty (S-u)^+ du$ is equal to zero. We can write directly

$$\begin{aligned} 2\int_K^S (S-u)du &= 2S\left(u\Big|_K^S\right) - 2\left(\frac{u^2}{2}\Big|_K^S\right) \\ &= 2S(S-K) - 2\left[\frac{S^2-K^2}{2}\right] = (S-K)^2 = (S-K)_+^2 \end{aligned} \tag{2.32}$$

Hence, here we conclude that

$$(S-K)_+^2 = 2\int_K^\infty (S-u)^+ du = 2\int_K^\infty (S_\tau - y)dy \tag{2.33}$$

.Finally, if we take an expectation star of both sides in Equation 2.33;

$$E^\star[(S_\tau - K)_+^2] = 2\int_K^\infty E^\star[(S_\tau - y)]dy = 2\int_K^\infty C(\tau, K)dy \tag{2.34}$$

.

Step 5: Let $f_0(x) = (x_+)^2$ and, for $\epsilon > 0$,

$$f_\epsilon(x) = \begin{cases} 0 & \text{if } x < 0 \\ \frac{x^3}{3\epsilon} & \text{if } x \in [0, \epsilon] \\ x^2 - \epsilon x + \frac{\epsilon^2}{3} & \text{if } x > \epsilon \end{cases}$$

(a) First we should prove that, for $\epsilon > 0$,f_ϵ is of class C^2, that $lim_{\epsilon \to 0}(f_\epsilon) = f_0(x)$ for every $x \in R$, and that $\forall x \geq 0$, $0 \leq f\epsilon(x) \leq f_0(x)$,$0 \leq f'_\epsilon(x) \leq 2x$,$0 \leq f''_\epsilon(x) \leq 2$:

To begin with, to prove that f_ϵ is of class C^2 , we need show that left and right limits at 0 and ϵ is equal to each other on functions $f_\epsilon(x)$,$f'_\epsilon(x)$,and $f''_\epsilon(x)$. To do so, we find $f'_\epsilon(x)$, and $f''_\epsilon(x)$ as below:

$$f'_\epsilon(x) = \begin{cases} 0 & \text{if } x < 0 \\ \frac{x^2}{\epsilon} & \text{if } x \in [0, \epsilon] \\ 2x - \epsilon & \text{if } x > \epsilon \end{cases}, \quad f''_\epsilon(x) = \begin{cases} 0 & \text{if } x < 0 \\ \frac{2x}{\epsilon} & \text{if } x \in [0, \epsilon] \\ 2 & \text{if } x > \epsilon \end{cases}$$

Now, let us look left and right limits:

$$lim_{x \to 0^-}\left(f_\epsilon(x) = 0\right) = 0 = lim_{x \to 0^+}\left(f_\epsilon(x) = \frac{x^3}{3\epsilon}\right)$$

$$lim_{x \to \epsilon^-}\left(f_\epsilon(x) = \frac{x^3}{3\epsilon}\right) = \frac{\epsilon^2}{3} = lim_{x \to \epsilon^+}\left(f_\epsilon(x) = x^2 - \epsilon x + \frac{\epsilon^2}{3}\right)$$

$$lim_{x \to 0^-}\left(f'_\epsilon(x) = 0\right) = 0 = lim_{x \to 0^+}\left(f'_\epsilon(x) = \frac{x^2}{\epsilon}\right)$$

$$lim_{x \to \epsilon^-}\left(f'_\epsilon(x) = \frac{x^2}{\epsilon}\right) = \epsilon = lim_{x \to 0^+}\left(f'_\epsilon(x) = 2x - \epsilon\right)$$

$$lim_{x \to 0^-}\left(f''_\epsilon(x) = 0\right) = 0 = lim_{x \to 0^+}\left(f''_\epsilon(x) = \frac{2x}{\epsilon}\right)$$

$$lim_{x \to \epsilon^-}\left(f''_\epsilon(x) = \frac{2x}{\epsilon}\right) = 2 = lim_{x \to \epsilon^+}\left(f''_\epsilon(x) = 2\right)$$

Since all left and right limits are equal as above, we say that f_ϵ is of class C^2.
Let us now compute $lim_{\epsilon\to 0}(f_\epsilon)$.

$$\lim_{\epsilon\to 0}\left(f_\epsilon(x)=\begin{cases}0 & \text{if } x<0\\ \frac{x^3}{3\epsilon} & \text{if } x\in[0,\epsilon]\\ x^2-\epsilon x+\frac{\epsilon^2}{3} & \text{if } x>\epsilon\end{cases}\right)$$
$$=\begin{cases}lim_{\epsilon\to 0}0=0 & \text{if } x<0\\ lim_{\epsilon\to 0}\frac{x^3}{3\epsilon}=0 & \text{if } x=0\\ lim_{\epsilon\to 0}x^2-\epsilon x+\frac{\epsilon^2}{3}=x^2 & \text{if } x>0.\end{cases}$$

Thus the above limit equals to:

$$\begin{cases}0 & \text{if } x\le 0\\ x^2 & \text{if } x>\epsilon\end{cases}=(x_+)^2$$

Given $\epsilon>0$ and ϵ is so small. Then we have

$$f_0(x)-f_\epsilon(x)=\begin{cases}0 & \text{if } x<0\\ x^2-\frac{x^3}{3\epsilon}>0 & \text{if } x\in[0,\epsilon]\ge 0\\ \epsilon x+\frac{\epsilon^2}{3}>0 & \text{if } x>\epsilon\end{cases}\quad\forall x$$

Therefore, $\forall x\ge 0$, $0\le f\epsilon(x)\le f_0(x)$.Also,

$$2x-f'_\epsilon(x)=\begin{cases}2x & \text{if } x<0\\ 2x-\frac{x^2}{\epsilon}=x(2-\frac{x}{\epsilon})>0 & \text{if } x\in[0,\epsilon]\ge 0\\ 2x-(2x-\epsilon)=\epsilon>0 & \text{if } x>\epsilon\end{cases}\quad\forall x$$

Therefore,$\forall x\ge 0$,$0\le f'_\epsilon(x)\le 2x$.Also,

$$2-f''_\epsilon(x)=\begin{cases}2 & \text{if } x<0\\ 2-\frac{2x}{\epsilon}=2(1-\frac{x}{\epsilon})>0 & \text{if } x\in[0,\epsilon]\ge 0\\ 0 & \text{if } x>\epsilon\end{cases}\quad\forall x$$

Therefore, $\forall x\ge 0$,$0\le f''_\epsilon(x)\le 2$.

(b) Secondly, we should prove that, for $K\ge 0$ and $\tau\in[0,\tilde{\tau}]$,

$$E^\star[f_\epsilon(S_\tau-K)]=f_0(S_0-K)+\frac{1}{2}E^\star\left[\int_0^\tau f''_\epsilon(S_0-K)S_u^2\sigma^2(u,S_u)du\right]$$

Using Ito's formula on the function $f_\epsilon(S_\tau-K)$, we have

$$f_\epsilon(S_\tau-K)=f_\epsilon(S_0-K)+\int_0^\tau f'_\epsilon(S_0-K)dS_u+\frac{1}{2}\int_0^\tau f''_\epsilon(S_0-K)d\langle S\rangle_u \quad . \text{ (2.35)}$$

When we rewrite Equation 2.35 by substituting the explicit expressions for dS_u and $d\langle S\rangle_u$ we get

$$f_\epsilon(S_\tau - K) = f_\epsilon(S_0 - K) + \int_0^\tau f'_\epsilon(S_0 - K)S_u\sigma(u, S_u)dW_u \tag{2.36}$$

$$+ \int_0^\tau f'_\epsilon(S_0 - K)S_u\mu(u)du + \frac{1}{2}\int_0^\tau f''_\epsilon(S_0 - K)S_u^2\sigma^2(u, S_u)du \tag{2.37}$$

Taking $E^\star$ of Equation 2.36 we get

$$E^\star[f_\epsilon(S_\tau - K)] = E^\star[f_\epsilon(S_0 - K)] + E^\star\left[\int_0^\tau f'_\epsilon(S_0 - K)S_u\sigma(u, S_u)dW_u\right]$$
$$+E^\star\left[\int_0^\tau f'_\epsilon(S_0 - K)S_u\mu(u)du\right] + E^\star\left[\frac{1}{2}\int_0^\tau f''_\epsilon(S_0 - K)S_u^2\sigma^2(u, S_u)du\right]$$

Since $E^\star$ of Brownian Motion is martingale, we can eliminate that term. Also, since $\mu(t)$ is given 0, that term having $\mu(t)$ in it is 0. Therefore, we get what desire,i.e.,

$$E^\star[f_\epsilon(S_\tau - K)] = E^\star[f_\epsilon(S_0 - K)] + \frac{1}{2}E^\star\left[\int_0^\tau f''_\epsilon(S_0 - K)S_u^2\sigma^2(u, S_u)du\right] \tag{2.38}$$

Final Step: Assume that, for every $t \in (0, \tilde{\tau}]$, the random variable S_t has, under probability $P^\star$, a density p(t,.), where $(t, x) \to p(t, x)$ is continuous on $(0, \tilde{\tau}] \times R^+$.

(a) Firstly, we prove that, for $0 < \tau \leq \tilde{\tau}$ and $K > 0$, $p(\tau, K) = \left(\frac{\partial^2 C}{\partial K^2}(\tau, K)\right)$:

We know from 4(d):

$E^*[(S_\tau - K)_+^2] = 2\int_K^\infty C(\tau, y)dy$

Now, we take three times derivatives of both sides of the equation with respect to K to prove the statement above. To clarify the solution, we show derivatives one by one,i.e.,

<u>First Derivative:</u>

$$\begin{aligned}\frac{\partial}{\partial K}E^*[(S_\tau - K)_+^2] &= \frac{\partial}{\partial K}\left[\int (y - K)_+^2 p(\tau, y)dy\right] \\ &= \frac{\partial}{\partial K}\left[\int_K^{+\infty} (y - K)^2 p(\tau, y)dy\right]\end{aligned} \tag{2.39}$$

Since integral's end point contains a function of K, we need to apply Liebniz Rule. To do so, let $g(y, K) = (y - K)^2$.Then

$$
\begin{aligned}
-g(y,K)\frac{\partial}{\partial K}(K) + \left[\int_K^{+\infty} \frac{\partial}{\partial K}((y-K)^2)p(\tau,y)dy\right] \\
= -(y-K)^2 - 2\left[\int_K^{+\infty}(y-K)p(\tau,y)dy\right]
\end{aligned}
\tag{2.40}
$$

Second Derivative:

Again, since integral's end point contains a function of K, we need to apply Liebniz Rule To do so, let h(h,K)=(y-K). Then

$$
\begin{aligned}
&\frac{\partial}{\partial K}\left[-(y-K)^2 - 2\int_K^{+\infty}(y-K)p(\tau,y)dy\right] \\
&= -2(y-K) - 2\left[-h(y,K)\frac{\partial}{\partial K}(K) + \int_K^{+\infty}\frac{\partial}{\partial K}(y-K)p(\tau,y)dy\right] \\
&= -2(y-K) + 2(y-K) + 2\int_K^{+\infty} p(\tau,y)dy \\
&= 2\int_K^{+\infty} p(\tau,y)dy
\end{aligned}
\tag{2.41}
$$

Third Derivative:

Here, it is simply the usage of Fundamental Theorem of Calculus we have

$\frac{\partial}{\partial K}\left[\int_K^{+\infty} p(\tau,y)dy\right] = 2p(\tau,K)$

In conclusion, we showed above that

$\frac{\partial^3}{\partial K^3}[E^*[(S_\tau - K)_+^2]] = 2p(\tau,K)$

First Derivative:

$\frac{\partial}{\partial K}\left[2\int_K^{+\infty} C(\tau,y)dy\right] = 2C(\tau,K)$

Second and Third Derivative:

$\frac{\partial^2}{\partial K^2}(2C(\tau,K)) = 2\frac{\partial^2 C}{\partial K^2}(\tau,K)$

In conclusion, we showed above that

$\frac{\partial^3}{\partial K^3}\left[2\int_K^{+\infty} C(\tau,y)dy\right] = 2\frac{\partial^2 C}{\partial K^2}(\tau,K)$

By cancelling 2 which is common on both sides of the equation, we proved that

$p(\tau, K) = \frac{\partial^2}{\partial K^2}(\tau, K)$

(b) Secondly, we should prove, using Question 5, that

$E^{\star}[(S_\tau - K)_+]^2 = (S_0 - K)_+^2 + \int_0^\tau \left(\int_K^\infty y^2\sigma^2(u, y)p(u, y)dy\right) du$:

Since we already proved 5(b), we can directly use it to prove the above statement. Thus,we have

$E^*[f_\epsilon(S_\tau - K)] = f_\epsilon(S_0 - K) + \frac{1}{2}E^*\left[\int_0^\tau f_\epsilon^{''}(S_0 - K)S_u^2\sigma^2(u, S_u)du\right]$

Now, we take limits of both sides when $\epsilon \to 0$.In other words;

Taking Limit of LHS:

Using the Dominated Convergence Theorem we put the limit inside of the E^*.Thus, we have

$\lim_{\epsilon\to 0}(E^*[f_\epsilon(S_\tau - K)]) = E^*[\lim_{\epsilon\to 0} f_\epsilon(S_\tau - K)] = E^*[f_0(S_\tau - K)] = E^*[(S_\tau - K)_+^2]$

Taking Limit of RHS:

Here, we need to write the term of E^* in an explicit form. To do so, we use given density function $p(t, .)$.Also, we use again the Dominated Convergence Theorem to put E^* and the limit inside of the integral. Thus, we have

$$\begin{aligned}
&\lim_{\epsilon\to 0}\left[f_\epsilon(S_0) + \frac{1}{2}E^*\left[\int_0^\tau f_\epsilon^{''}(S_0 - K)S_u^2\sigma^2(u, S_u)du\right]\right] \\
&= \lim_{\epsilon\to 0}[f_\epsilon(S_0 - K)] + \lim_{\epsilon\to 0}\left[\frac{1}{2}E^*\left[\int_0^\tau f_\epsilon^{''}(S_0 - K)S_u^2\sigma^2(u, S_u)du\right]\right] \\
&= f_0(S_0 - K) + \frac{1}{2}\int_0^\tau E^*\left[\lim_{\epsilon\to 0}(f_\epsilon^{''}(S_0 - K)S_u^2\sigma^2(u, S_u))\right] du \qquad (2.42) \\
&= (S_0 - K)_+^2 + \frac{1}{2}\int_0^\tau \left(\int_K^{+\infty} 2y^2\sigma^2(u, y)p(u, y)dy\right) du \\
&= (S_0 - K)_+^2 + \int_0^\tau \left(\int_K^{+\infty} y^2\sigma^2(u, y)p(u, y)dy\right) du
\end{aligned}$$

In conclusion, when we take limits of both sides of the equality holds again. Thus,we proved the statement in (b),i.e.,

$E^*[(S_\tau - K)_+^2] = (S_0 - K)_+^2 + \int_0^\tau \left(\int_K^{+\infty} y^2\sigma^2(u,y)p(u,y)dy \right) du$

(c) Finally, we deduce from above that $\frac{\partial C}{\partial K}(K,\tau) = \frac{K^2\sigma^2(\tau,K)}{2}\frac{\partial^2 C}{\partial K^2}(\tau,K)$ (for $0 < \tau \leq \tilde{\tau}$ and $K > 0$):

Here,we use the statement 6(b) to prove the given statement so that we take two times derivative of 6(b) and multiply it with $\frac{1}{2}$. Now, we need to show LHS and RHS of the equality seperately. Thus, we have,

For LHS:

$$\begin{aligned} \frac{\partial}{\partial\tau}[E^*[(S\tau - K)_+^2]] =& 2E^*[(S_\tau - K)|+^*] = 2C(\tau,K) \\ &= \frac{1}{2}\frac{\partial}{\partial\tau}[2C(\tau,K)] = \frac{\partial C}{\partial\tau}(\tau,K) \end{aligned} \tag{2.43}$$

This simply means that

$$\frac{1}{2}\frac{\partial^2}{\partial\tau^2}[E^*[(S_\tau - K)_+^*]] = \frac{\partial C}{\partial\tau}(\tau,K)$$

For RHS:

Here, we use the Fundamental Theorem of Calculus so we have

$$\begin{aligned} &\frac{\partial}{\partial\tau}\left[(S_0 - K)_+^2 + \int_0^\tau \left(\int_K^{+\infty} y^2\sigma^2(u,y)p(u,y \right) du\right] \\ &\quad = \frac{\partial}{\partial\tau}\left[\int_0^\tau \left(\int_K^{+\infty} y^2\sigma^2(u,y)p(u,y)dy(\right) du\right] \\ &\quad = \int_K^{+\infty} y^2\sigma^2(\tau,y)p(\tau,y)dy \end{aligned} \tag{2.44}$$

Taking one more derivative and using again the Fundamental Theorem of Calculus and 6(a), we have

$$\frac{1}{2}\frac{\partial}{\partial\tau}\left[\int_K^{+\infty} y^2\sigma^2(\tau,y)p(\tau,y)dy\right] = \frac{K^2\sigma^2(\tau,K)}{2}p(\tau,K) = \frac{K^2\sigma^2(\tau,K)}{2}\frac{\partial^2 C}{\partial K^2}(\tau,K) \tag{2.45}$$

Since RHS is equal to LHS,we get:

$$\frac{\partial C}{\partial \tau}(\tau, K) = \frac{K^2 \sigma^2(\tau, K)}{2} \frac{\partial^2 C}{\partial K^2}(\tau, K), \tag{2.46}$$

which is called **Dupire's Equation**.

CHAPTER 3

Hedging and Pricing Using Historical Fit

In this chapter, we fit the local volatility model to BIST30 using historical price data of the BIST30 index directly; then we use these fits to price and hedge European options on BIST30. We do these over two periods: 15.01.2016-05.02.2016 (two weeks, we will refer to this time interval as the "January period") and 01.03.2016-31.03.2016 (four weeks, will be referred to as the "March period.").

3.1 The fit

As indicated in the introduction, for the purposes of this chapter we assume the local volatility function to depend on the stock price only and to be piecewise linear in $\log(S_t)$; these are simplifying assumptions and can be relaxed in future work. Here we would like to point out that there are many earlier works estimating local volatility models from data, see, e.g., [8, 2], it is worth looking into these approaches within the present context, this may be undertaken in future work.

To perform the fit we proceed as follows: to fit a local volatility model on day t, we take the price data of the 200 days preceding day t; let m denote the minimum value of $\log(S_t)$ observed in these 200 days and let M denote the maximum. We divide the interval (m, M) into 3 bins of equal size. Then we compute the returns for each day and classify them into the 3 bins according to the value of the index for which the return is computed. Then the volatility of each bin is computed separately; t o get our local volatilility function the computed volatilities are connected with lines. Finally, outside of the interval (m, M) the local volatility function is taken constant in such a way to make it continuous. In other words, we assume $\sigma(t, x) = \sigma(x)$ which means that σ depends on only $x = log(S)$. We further assume;

$$\begin{aligned} \sigma(x) = a_i x + b_i, x_i \in (c_{i-1}, c_i) \\ \sigma(x) = l, x \leq m \\ \sigma(x) = r, x \geq M \\ m = c_0 < c_1 < ..... < c_k = M \end{aligned} \tag{3.1}$$

Here $k - 1$ is the number of bins; a_i, b_i, l, r are such that σ is a continous function.

Let us comment on the two parameters: the length of the history used in the computation (taken to be 200 above) and the number of bins (3): based on our numerical experiments, these parameters seem to have limited impact on the hedging and pricing results. We have chosen the length 200 because it represents approximately one year of price history. As for the number of bins: with increasing number of bins the model becomes more general. Our numerical experiments indicate that after 3 the hedging and pricing results seem to barely change with increasing number of bins and 3 bins appear to give a general enough model under the current assumptions. A more systematic study of the effect of these parameters on the pricing and hedging results may be undertaken in future work.

3.1.1 The local volatility fit for the January period

The local volatility for BIST30 estimated for the January period is shown in Figure 3.2; for comparison the constant Black Scholes volatility (again estimated using historical volatility) is shown in Figure 3.1. Both of these figures display a graph for each week of the given period: the later the week, the thicker the line representing that week's estimated local volatility.

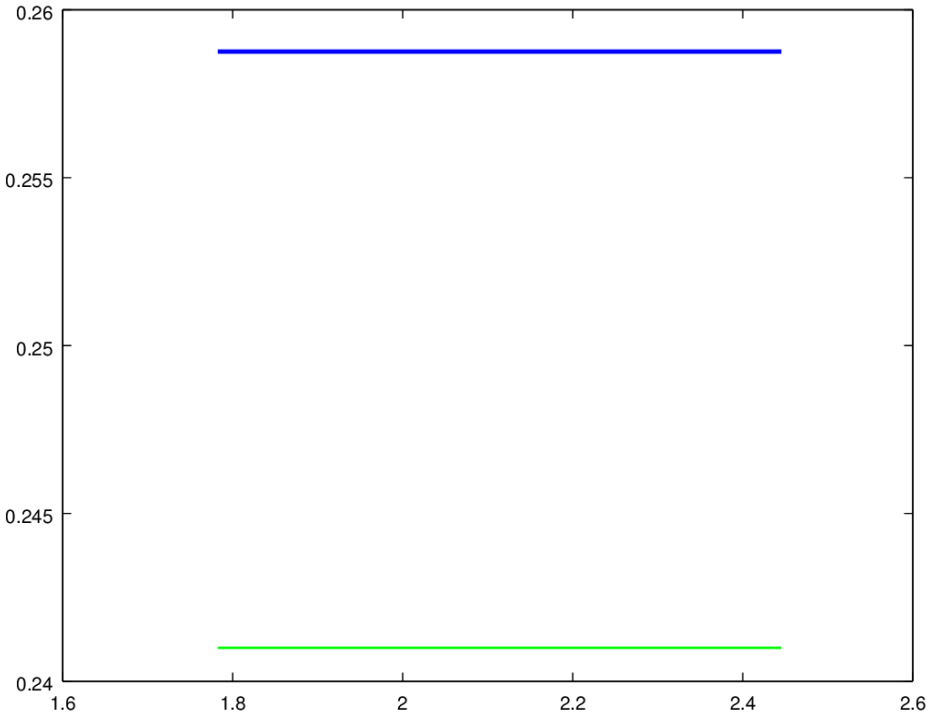

Figure 3.1: Black-Scholes Volatility in 15.01.2016-05.02.2016

Concerning these fits we observe the following: the shape of the local volatility curve

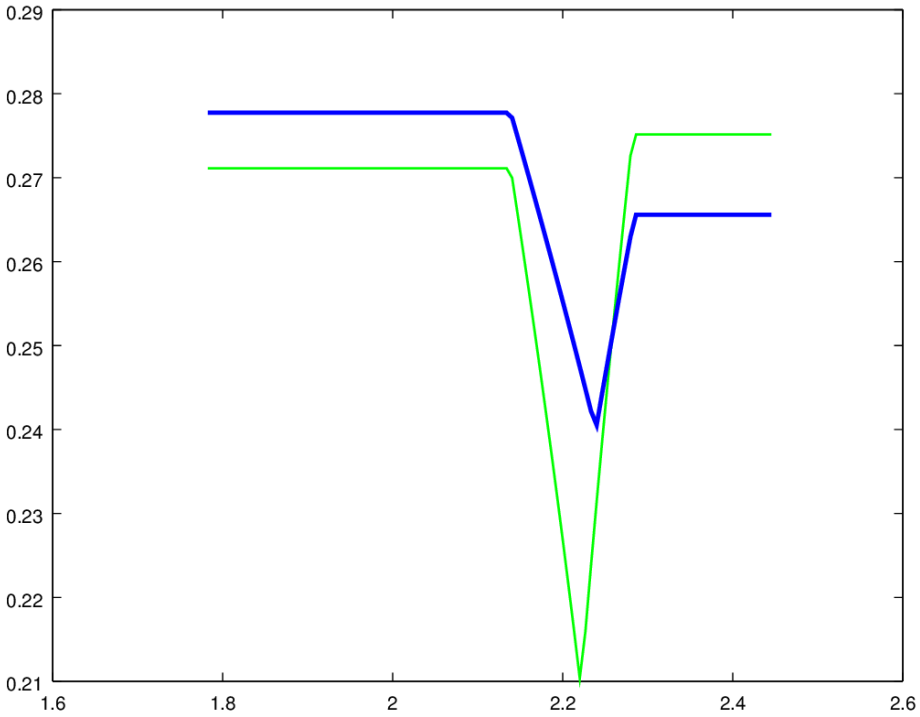

Figure 3.2: Local Volatility in 15.01.2016-05.02.2016

doesn't change in these two weeks but their values slightly change. The Black scholes constant volatility alsochanges slightly in the two weeks covered.

3.1.2 The local volatility fit for March period

The local volatility for BIST30 estimated for the March period is shown in Figure 3.4; for comparison the constant Black Scholes volatility (again estimated using historical volatility) is shown in Figure 3.3. As in the previous subsection, both of these figures display a graph for each week of the given period (the length of the period covered is slightly longer than four weeks, therefore Figure 3.3 gives a fifth estimate): the later the week for which the fit is estimated, the thicker the line representing the estimated local volatility. We note that as the weeks progress the shape of the local volatility fit changes.

3.2 Pricing BIST30 Warrants using Historical Data

The next subsection reviews how one computes option prices using the local volatility model. Subsection 3.2.2 computes actual prices of several call warrants written on

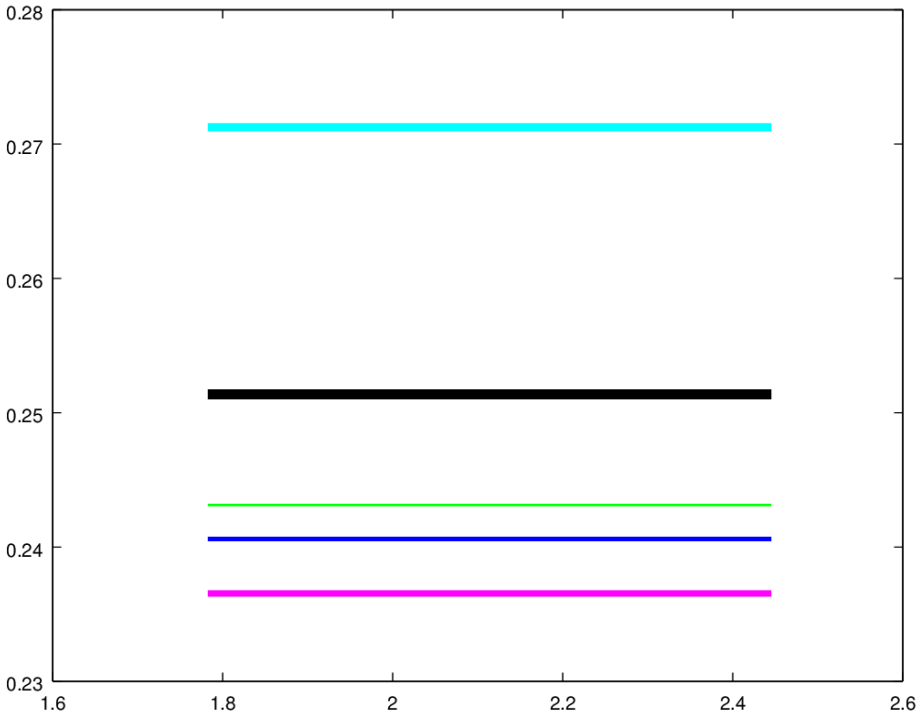

Figure 3.3: Black-Scholes Volatility in 01.03.2016-31.03.2016

BIST30 using the local volatility models estimated in the previous section and using the computational approach explained in subsection 3.2.1. For the pricing example, we slightly extend the periods we study: we will give two pricing examples from January, two from February, two from March and two from April. The local volatility models for the dates not covered in the previous section are estimated using exactly the same methods as of the previous section.

3.2.1 Computation of the option price

Consider a call option with strike K and maturity T; as reviewed in the previous chapter, its price will be

$$V(s,t) \doteq \mathbb{E}_s \left[e^{-r(T-t)} (S_T - K)^+ \right],$$

where S_t has the dynamics given in Equation 2.3. If we change our price variable to $x = \log(s)$ and define $X_t = \log(S_t)$ one can write the last display as

$$V(x,t) = \mathbb{E}_x \left[e^{-r(T-t)} (e^{X_T} - K)^+ \right].$$

In the BS framework σ is a constant and the last expectation can be written as a one dimensional integral against the normal distribution. When σ is not constant we no

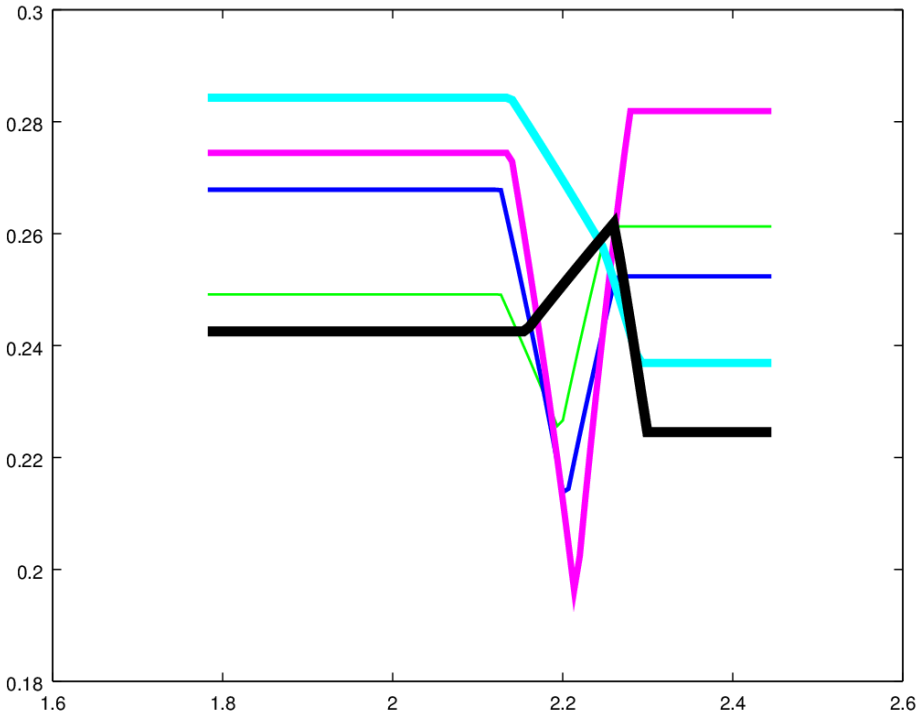

Figure 3.4: Local Volatility in 01.03.2016-31.03.2016

longer have such explicit formulas. An alternative and standard approach to the comptuation of the same expectation is by solving the partial differential equation (PDE) satisfied by V, derived in the previous chapter the function C (as a function of x and t:

$$V_t + \sigma^2(t,s)V_{xx}/2 + (r - \sigma^2(t,s)/2)V_x = 0,$$

with the terminal condition

$$V(T,x) = (e^x - K)^+. \tag{3.2}$$

This PDE doesn't have straightforward closedform expressions for its solution but its solution via numerical techniques is standard. For the purposes of this thesis we have used the Markov chain approximation technique given in [12]. This involves the discretization of the space and time variables to construct a discrete time and space Markov chain X^n whose transition probabilities approximate the diffusion Equation 2.3. For the local volatility model the dynamics of X^n are given as follows:

$$X_0^n = x, X_{k+1}^n = X_k^n + I_k^n \Delta x$$

where I_k takes values in $\{-1, 0, 1\}$. Let $\mathcal{F}_k \doteq (X_1, X_2, ..., X_k)$; the conditional distribution of I_n given $\mathcal{F}_n$ is

$$P(I_{k+1} = 1|\mathcal{F}_n) = 0.5(\sigma(X_k)^2 + \gamma\Delta x); P(I_{k+1} = 0|\mathcal{F}_n) = 1 - \sigma(X_k)^2$$

where

$$\gamma = r - \sigma(X_n)^2/2$$

and Δx is the discrete space step size. Let Δt be the time step used in the discretization; then it will take X^n $N = T/\Delta_t$ steps to reach maturity. The resulting approximation of the option prices consists of the expectation

$$C^n(x,T) = e^{-rT}\mathbb{E}\left[\left(e^{X_N^n} - K\right)^+\right].$$

Because X^n is discrete and takes only N steps the last expectation can be computed by backward recursion in finitely many steps. As n grows and $\Delta x, \Delta t \to 0$ the time and space grids are refined and the discrete markov chain X^n converges weakly to $\log(S_t)$. For further details of the construction of the discrete time process X^n and convergence proofs we refer the reader to [12].

3.2.2 Application to data

For January and February, for our call warrants, we take the strikes 90 and 95 and the maturities 29.02.2016 and 29.04.2016. All of these warrants were among the highly traded warrants written by Deutsche Bank in January and February of 2016[1] the availability of their market price will give us a chance to compare model and market prices. The first part of Table 3.1 show the model prices on 15.01.2016, 20.01.2016, 01.02.2016 and 16.02.2016. For March and April, we take 100 and 105 as strikes and 29.04.2016 and 30.06.2016 for the maturities; once again all of these warrants were available for trade in Borsa Istanbul in March and April. The second part of Table 3.1 show the prices of these options on 03.03, 11.03, 05.04, and 18.04.

A comparison of the local volatility model prices and BS prices listed in Table 3.1 is shown in Figure 3.5; we see that except for the first 6 prices the local volatilty model implies greater or equal prices as compared to BS.

The scatter plot of differences between model and market prices (computed with the formula $(P_{market} - P_{model})/P_{model}$) is given in Figure 3.6; Figure 3.7 gives the histogram of the same errors. It is clear from these figures that, for the examples covered by them, the market prices are almost always more expensive (up to 5 times) compared to the prices given by the local volatility model.

3.2.3 Hedging BIST30 Warrants

For the hedging, we use the delta hedging algorithm implied by the model. The self financing hedging portfolio is (B_t, D_t) where B_t is the bond position at time t and D_t is the delta position taken on the underlying stock. These are computed as follows:

$$D_t = \frac{\partial C}{\partial s}(t, S_t), B_t = e^{-rt}(C(t,S_t) - D_t S_t)$$

[1] Other european call warrants written by the same market maker on BIST30 and traded in the same period had strikes 100, 105, 110, 115 and 120; the value of the index in January and February was around $85-90$ thus the strikes we use are the ones closest to being at the money among those written at the time.

Date, Index	Maturity	Strike	Market	Model	BS
15.01, $S = 86.95$	29.02	90	2.43	1.23	1.88
		95	0.93	0.25	0.64
	29.04	90	4.23	2.76	3.90
		95	2.38	1.16	2.16
20.01, $S = 85.12$	29.02	90	1.58	0.61	1.82
		95	0.53	0.088	0.67
	29.04	90	3.38	1.94	0.53
		95	1.83	0.73	0.07
01.02, $S = 89.95$	29.02	90	2.98	1.96	1.94
		95	1.03	0.36	0.34
	29.04	90	5.15	3.82	3.89
		95	2.93	1.74	3.89
16.02, $S = 87.1$	29.02	90	0.78	0.79	0.25
		95	0.13	0.31	0.0034
	29.04	90	3.23	2.06	2.005
		95	1.58	0.68	0.66
03.03, $S = 94.34$	29.04	100	1.53	0.95	0.73
		105	0.68	0.24	0.15
	30.06	100	3.18	2.34	1.93
		105	1.89	1.04	0.77
11.03, $S = 97.84$	29.04	100	2.23	1.90	1.65
		105	0.83	0.54	0.40
	30.06	100	4.23	3.71	3.28
		105	2.38	1.80	1.47
05.04, $S = 101.80$	29.04	100	3.75	3.11	2.98
		105	1.28	0.76	0.63
	30.06	100	6.3	5.21	4.95
		105	3.78	2.09	2.33
18.04, $S = 105.91$	29.04	100	6.43	6.17	6.16
		105	2.53	1.95	1.85
	30.06	100	9.03	7.95	1.80
		105	5.75	4.39	4.18

Table 3.1: Prices (computed using local volatility and those observed in the market) of several options in the first four months of 2016; the first column gives the date (all from 2016) when the prices are computed and the value of BIST30 on that date

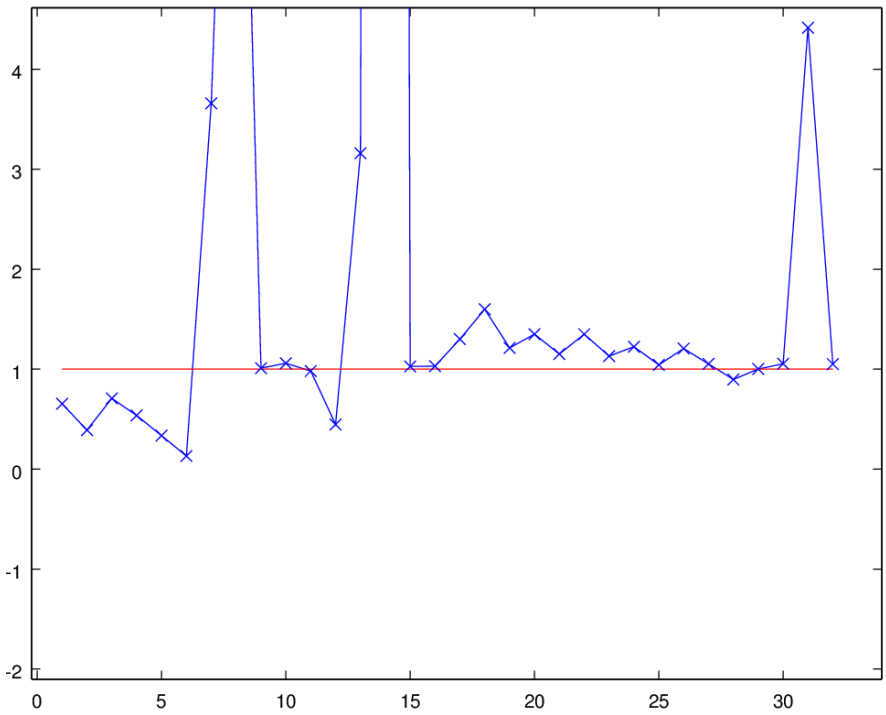

Figure 3.5: P_{model}/P_{BS} for the prices given in Table 3.1

where $\frac{\partial C}{\partial s}$ is the delta of the option, i.e., the derivative of the price with respect to the price of the underlying. A well known fact is that a hedging portfolio thus constructed is self financing and its value at time T equals exactly the payoff of the option [13]. To practically implement the hedging algorithm we discretize it; because the price data we have is daily our stepsize will be a day. Thus the hedging portfolio is updated once at the end of the trading day. This discretization and model error will lead to a hedging error, i.e., the hedging portfolio will no longer be self financing. We keep track of the hedging error using the following equations:

$$H_0 = 0, H_{t+1} = e^{-r/365} H_t + B_t e^{r(t+1)} + D_t S_{t+1} - C_{t+1};$$

H_t is the cost of running the hedging algorithm upto day t; in a perfect hedge we would have $H_t = 0$. We will refer to $100H_t/C_t$ is hedging error expressed as a percentage of the current call value. This will be our main measure of the performance of the hedging algorithm.

3.2.4 Hedging with model prices

When a historical fit is done, a choice arises as to which prices to use in the hedging algorithm. This subsection runs the hedging algorithm with model prices in the January and March periods. For the January period we take the strike of our call to be $K = 90$

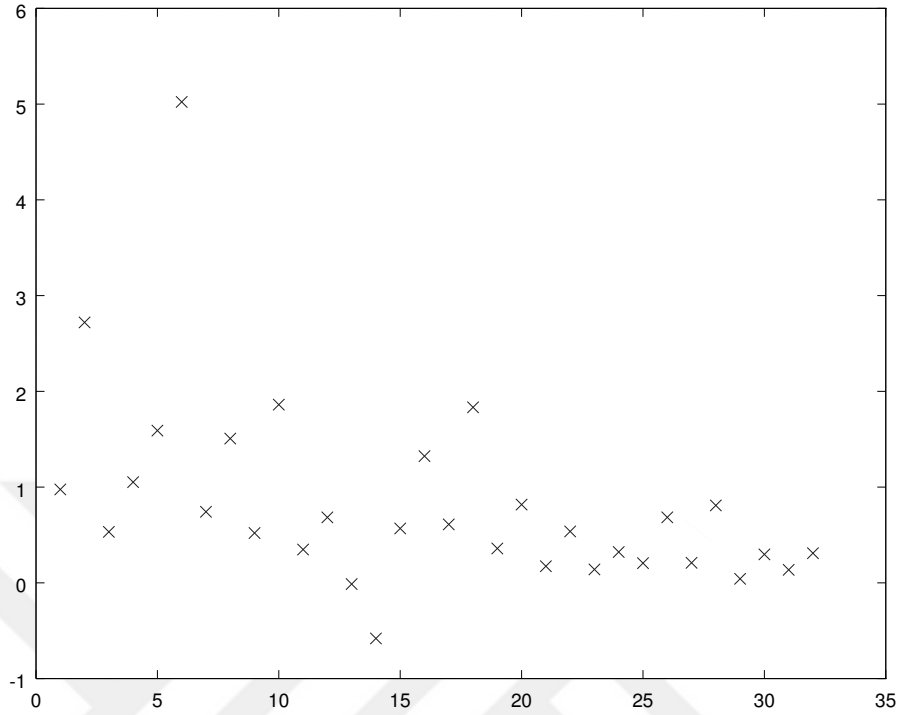

Figure 3.6: The price difference between market and model prices given in Table 3.1; $((P_{market} - P_{model})/P_{model})$

and its maturity 29.02. For the March period we take the strike $K = 95$ and maturity 29.04. The hedging errors for these warrants are shown in Figures 3.8 and 3.9. The red line represents the hedging error of the local volatility hedging algorithm and the blue line represents that of Black Scholes.

In Figures 3.8 and 3.9, we see that in January, hedging with Black-Scholes Model and the Local Volatility Model act similar. However, Black-Scholes Model causes more loss especially in the last day of the period; the BS model realizes around 110% loss whereas the local volatility realizes around 80% loss. In March, on the other hand, both models act almost the same; both models realize around 90% loss.

3.2.5 Hedging with market prices

This subsection runs the same hedging algorithm now using the warrant prices observed in the market. For the purpose of this section we will run the hedging algorithm also on two different maturities: 29.02 and 29.04 for the January period; 29.04 and 30.06 for the March period. The hedge results for the January period are given in Figures 3.10 and 3.11.

For the March period the strike is $K = 95$ and maturities are 29.04 and 30.06. The

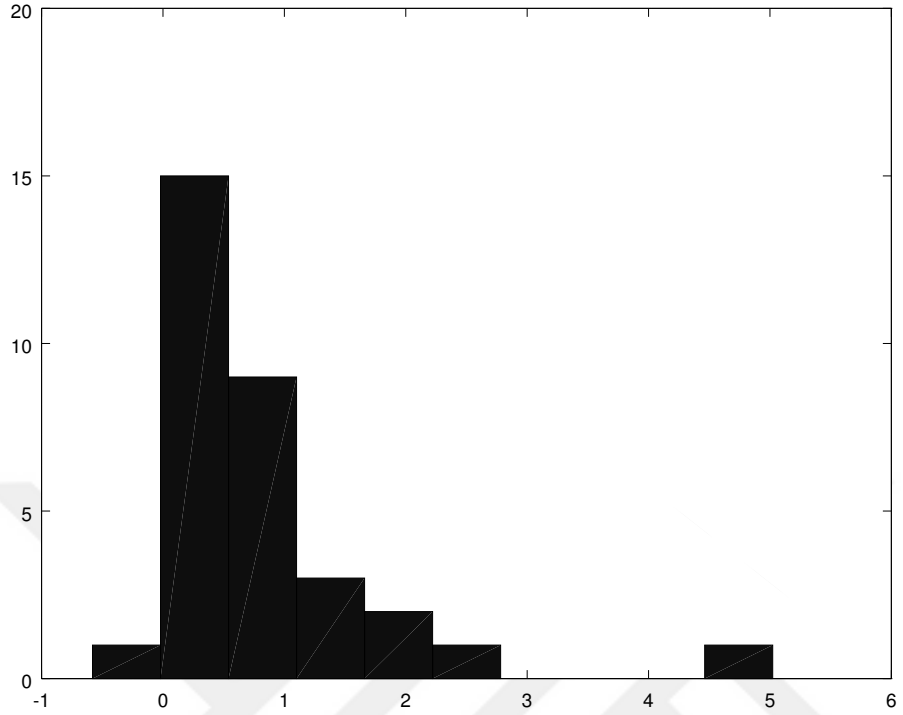

Figure 3.7: The histogram of the price differences given in Figure 3.6

hedging results are given in Figures 3.12 and 3.13.

Our comments on the results reported in these Figures are as follows: once the market prices are used, the difference observed in Figure 3.8 between BS hedge results and local volatility hedge results disappears (compare with Figure 3.10). In fact, in all of the hedges using market prices, there is little difference between the delta hedging of the BS model and that of the local volatility model. Finally, we observe that as compared to the results of the previous section, the hedge errors drop signficantly to around 20%. With this observation we can interpret the price difference observed in the previous chapter as follows: the local volatility models used in the present thesis underprices the call warrants studied in this thesis.

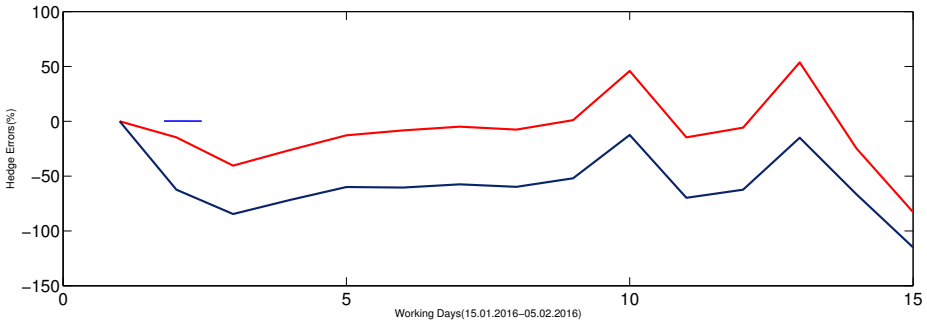

Figure 3.8: Hedging BIST30 Warrants with Therotical Prices in January

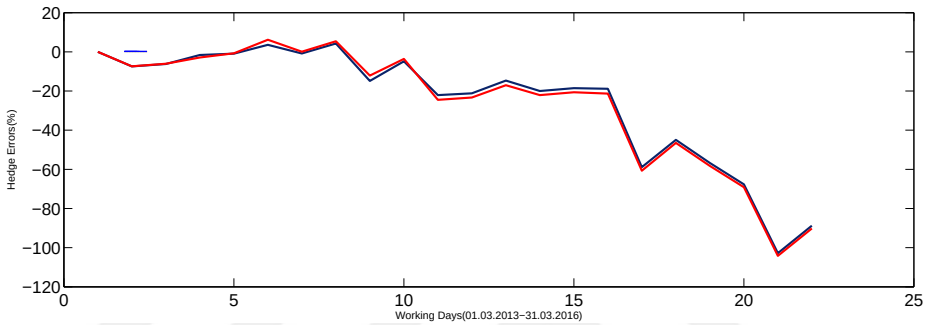

Figure 3.9: Hedging BIST30 Warrants with Theoretical Prices in March

Figure 3.10: Hedging error for $K = 90$ and maturity 29.02

Figure 3.11: Hedging error for $K = 90$ and maturity 29.04

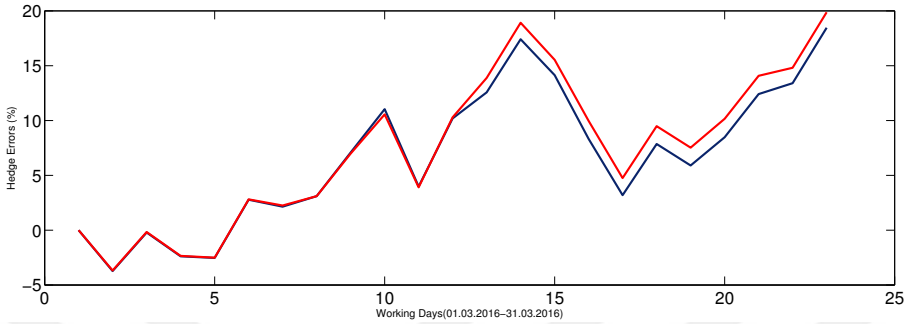

Figure 3.12: Hedging error for with $K = 95$ and maturity 29.04

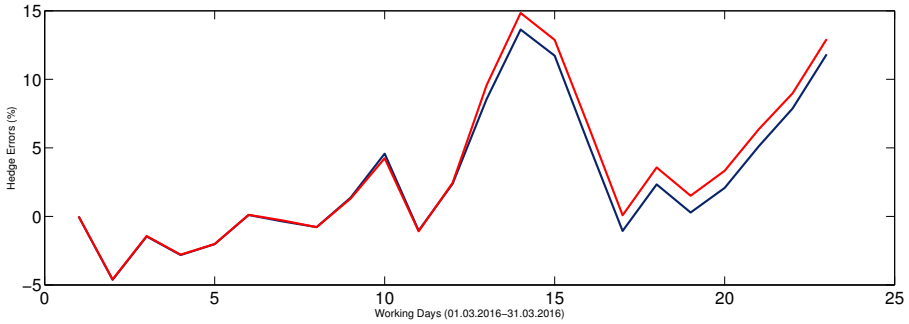

Figure 3.13: Hedging error for $K = 95$ and maturity 30.06

CHAPTER 4

Hedging with Local Volatility Implied by the Heston Model

4.1 Heston parameters and hedging performance

The Heston model is one of the first and most well known stochastic volatility models [9]. Its main advantage is the availability of closed form pricing formulas under it for basic European options.In the Heston Model [9], the underlying stock price S_t follows the Black-Scholes process with a stochastic variance v_t following Cox-Ingersoll-Ross process [3] which is actually an example of a square root process. Hence, the model is the bivariate system of stochastic differential equations (SDEs) [16]

$$dS_t = \mu S_t dt + \sqrt{v_t} S_t dW_t^{(1)}, \tag{4.1a}$$

$$dv_t = \kappa(\theta - v_t)dt + \sigma\sqrt{v_t} dW_t^{(2)}, \tag{4.1b}$$

where μ the drift of the process for the stock, $\kappa > 0$ the mean reversion speed for the variance, $\theta > 0$ the mean reversion level for the variance, and $\sigma > 0$ the volatility of the variance. Moreover, $W^{(1)}$ and $W^{(2)}$ are two Brownian motions such that $E^p[dW_t^{(1)} dW_t^{(2)}] = \rho dt$. In other words, $\rho \in [-1, 1]$ represents the correlation between $W^{(1)}$ and $W^{(2)}$. For more on this model and an implementation of fitting and pricing algorithms for the Heston model we refer the reader to [16].

As already indicated in the introduction an alternative way to fit a local volatility model to market prices, explained in [7], is to first fit a Heston model and then use Dupire's formula to get the local volatility. The goal of this section is to use the local volatility model obtained by such a fit to hedge two call warrants in the March period. Thus we propose the following hedging algorithm:

1. fit the Heston model to market prices,
2. use Equation 2.13 to derive a local volatility model from Heston model prices,
3. use the delta hedging algorithm, as described in subsection 3.2.3, using the delta of the pricing function computed from the local volatility model given by the heston model.

Dupire's formula implies that there is an extremely simple way to implement the above steps without actually computing the local volatility function itself: instead of the last two steps one simply computes the delta of the Heston model and uses it as the delta in the hedging algorithm of subsection 3.2.3. Figures 4.1 and 4.2 give the hedging error associated with this algorithm applied to two warrants in the March period: both warrants have strike $K = 95$ and they have the respective maturities 29.04 and 30.06; as in the previous section the red line gives the hedging error for the Heston-implied local volatility hedging algorithm and the blue line gives the hedging error of the Black scholes model. To apply the hedging algorithm we need to fit the Heston model to market data during the March period. This was already done in [14]; we quote the parameter fits listed in Table 4.1 from that work.

	κ	θ	σ	v_0	ρ
01.03.2016	6.3868	0.0489	0.3094	0.0702	0.9793
02.03.2016	12.3838	0.0612	0.8786	0.0710	0.3990
03.03.2016	19.9720	0.0561	0.4496	0.0677	0.9612
04.03.2016	2.0042	0.0000	0.3906	0.0695	0.9989
07.03.2016	1.2846	0.0023	0.2057	0.0696	0.9826
08.03.2016	1.6237	0.0001	0.2484	0.0662	-0.9988
09.03.2016	11.9639	0.0526	0.3830	0.0563	0.9934
10.03.2016	12.0781	0.0571	0.2971	0.0499	0.9935
11.03.2016	19.9748	0.0550	0.5111	0.0401	0.9974
14.03.2016	19.9638	0.0543	0.6892	0.0360	0.9948
15.03.2016	13.2286	0.0561	0.2704	0.0480	0.9858
16.03.2016	19.9847	0.0562	0.7625	0.0357	0.7337
17.03.2016	16.3918	0.0569	0.7249	0.0400	0.9988
18.03.2016	0.0604	1.9371	0.4819	0.0400	0.9990
21.03.2016	0.0860	1.5786	0.4335	0.0436	0.9989
22.03.2016	0.0858	0.0546	0.2071	0.0584	0.9979
23.03.2016	0.3991	0.0191	0.1428	0.0638	0.9963
24.03.2016	19.9552	0.0664	0.3502	0.0575	0.9947
25.03.2016	19.9274	0.0668	0.1605	0.0695	0.9739
28.03.2016	19.9751	0.0652	0.3750	0.0625	0.9924
29.03.2016	19.9928	0.0657	0.6282	0.0530	0.9984
30.03.2016	19.9938	0.0667	0.6559	0.0546	0.9988

Table 4.1: Heston Parameters

We note that the results reported in Figures 4.1 and 4.2 differ from those reported in subsection 3.2.5: the hedging error processes for the local volatility and BS algorithms no longer overlap (compare Figures 4.1 and 4.2 to those in subsection 3.2.5). The absolute value of the hedging error seem to be similar for the two hedging algorithms. At least for these two examples, the use of the Heston-implied local volatility seem to bring no futher gains in Hedging performance when compared to the simple BS.

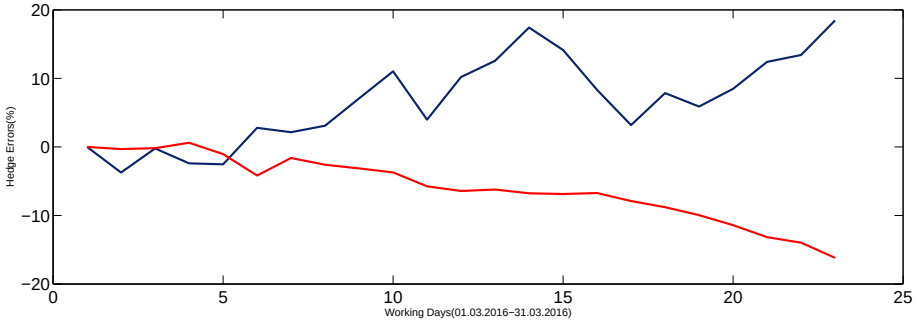

Figure 4.1: Hedge Errors in March- 29.04.2016

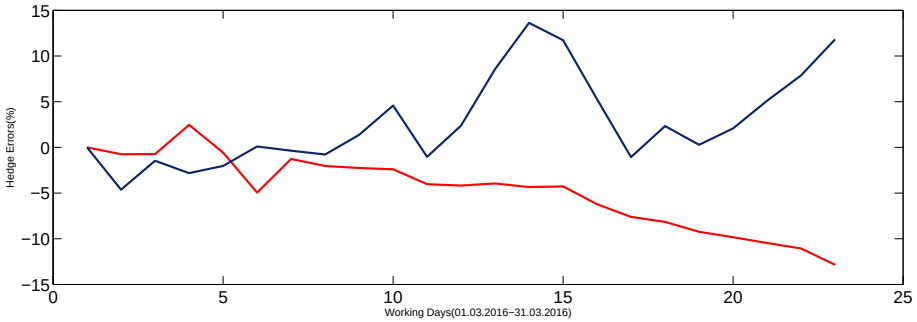

Figure 4.2: Hedge Errors in March- 30.06.2016

4.2 Approximation to Local Volalitility in the Heston Model

Dupire's formula allows one to derive a local volatility model from a Heston model. However, the quantities appearing Dupire's formula will in general require a nontrivial amount of computation. Note that in the estimates listed in Table 4.1 most of the time the ρ parameter takes values very close to 1 or -1. For these types of situations Gatheral developed a simple formula to compute the local volatility without computing explicitly all of the derivatives appearing in Dupire's formula. The goal of this section is to give a derivation of this formula; in this we follow [16].

We know that the Heston Model is established on two equations which are:

$$dS_t = \mu_t S_t dt + \sqrt{v_t} S_t dW^1 \tag{4.2a}$$

$$dv_t = \kappa(\theta - v_t)dt + \sigma\sqrt{v_t} dW^2 \tag{4.2b}$$

where μ the drift of the process for the stock, $\lambda > 0$ the mean reversion speed for the variance, $v_t > 0$ the mean reversion level for the variance, and $\eta > 0$ the volatility of the variance. Moreover, W^1 and W^2 are two Brownian motions such that $E^p[dW^1(t)dW^2(t)] = \rho dt$. In other words, $\rho \in [-1, 1]$ represents the correlation between W^1 and W^2.

The v process is a Cox-Ingersoll-Ross (CIR) model and for these models one can

explicitly compute the conditional expectation $E[v_t|v_s]$, $s < t$:

$$E[v_t|v_s] = (v_s - \theta)e^{-\kappa(t-s)} + \theta.$$

In particular $E[v_t|v_0]$ will be of use to us in the computations below, so let us define

$$\hat{v}_t = E[v_t|v_0] = (v_0 - \theta)e^{-\kappa t} + \theta. \tag{4.3}$$

In addition define

$$\hat{w}_t \doteq \int_0^t \hat{v}_s ds = (v_0 - \theta)\left(\frac{1 - e^{-\kappa t}}{\kappa}\right) + \theta t, \tag{4.4}$$

this is the "total" variance in the interval $[0, t]$.

Now set $x_t = \log(\frac{S_t}{K}) = f(S_t)$. If we use Ito's formula [13] to compute x_t directly,

$$f(S_t) = \log(\frac{S_t}{K}) = \log(\frac{S_0}{K}) + \int_0^t f'(S_s)dS_s + \frac{1}{2}\int_0^t f''d\langle S\rangle_s \tag{4.5}$$

Here, the quadratic variation of S_s is equal to $v_s S_s^2 ds$ from the equation (2.20a). If we plug f' and f'' and $d\langle S\rangle_s$, then our equation becomes:

$$f(S_t) = \log(\frac{S_0}{K}) + \int_0^t \frac{\frac{1}{K}}{\frac{S_s}{K}} dS_s + \frac{1}{2}\int_0^t -\frac{1}{S_s^2} v_s S_s^2 ds \tag{4.6}$$

Simplifying the last display gives

$$x_t = \log(\frac{S_0}{K}) + \int_0^t \frac{1}{S_s} dS_s - \frac{1}{2}\int_0^t v_s ds. \tag{4.7}$$

If we differentiate x_t, we get:

$$dx_t = \frac{1}{S_t} dS_t - \frac{v_t}{2} dt.$$

If we plug $dS_t = \mu_t S_t dt + \sqrt{v_t} S_t dW^1$ then we conclude that: (4.8)

$$dx_t = \frac{1}{S_t}(\mu_t S_t dt + \sqrt{v_t} S_t dW_t^1) - \frac{v_t}{2} dt$$

which is equal to

$$dx_t = \sqrt{v_t} dW_t^1 - \frac{v_t}{2} dt \tag{4.9}$$

One can represent W^1 and W^2 as linear combinations of two independent Brownian motions Z_t and B_t by defining $W_t^1 = B_t$ and $W_t^2 = \rho B_t + \sqrt{1 - \rho^2} Z_t$ where Z_t and B_t are orthogonal Brownian motions [16]. Then one can write dv_t as

$$dv_t = \kappa(\theta - v_t)dt + \sigma\sqrt{v_t}(\rho dZ_t + \sqrt{1 - \rho^2} dB_t) \tag{4.10}$$

If we assume $\rho \approx \pm 1$, then we obtain dv_t directly:

$$dv_t = \kappa(\theta - v_t)dt + \rho\sigma(dx_t + \frac{v_t}{2}dt). \tag{4.11}$$

Gatheral's approximation is based on the following ansatz:

Ansatz: $E[x_t|x_T] = \frac{x_T}{\hat{w_T}}\hat{w}_t$, where $\hat{w}$ is as in Equation 4.4.

Let $u_t = E[v_t|x_T]$ denote the expected value of the variance at time t conditional on x_T. Now, take the conditional expectation of Equation 4.11 and apply the ansatz to get:

$$du_t = \kappa(\theta - u_t)dt + \rho\sigma\left(\frac{x_T}{\hat{w_T}}\hat{v}_t dt + \frac{1}{2}u_t dt\right), \tag{4.12}$$

where $\hat{v}$ is as in Equation 4.3. Define $\kappa' = \kappa - \rho\sigma/2$ and $\theta' = \theta\kappa/\kappa'$. The last equation can be written as

$$\frac{du_t}{dt} + \kappa' u_t = \rho\sigma\frac{x_T}{\hat{w}_T}\hat{w}_t + \kappa'\theta'.$$

This is a first order linear ODE and it can be solved explicitly. Its solution at time T equals

$$u_T = \rho\sigma\frac{x_T}{\hat{w_T}}\int_0^T \hat{v}_t e^{\kappa'(T-t)}dt + \theta'(1 - e^{-\kappa' T}) + C_1 e^{\lambda' T}, \tag{4.13}$$

where C_1 is a constant to be determined from the initial condition $u_0 = \mathbb{E}[v_0|X_T] = v_0$. Setting $T = 0$ in the above equation implies that $u_0 = C_1 = v_0$. Then

$$u_T = \hat{v_T}' + \rho\sigma\frac{x_T}{\hat{w}_T}\int_0^T \hat{v}_t e^{-\kappa'(T-t)}dt \tag{4.14}$$

where $\hat{v}'_T = (v_0 - \theta)e^{-\kappa' T} + \theta'$. Finally, carrying out the integral appearing in the last display we arrive at Gatheral's approximation of local volatility via the Heston model:

$$u_T = \hat{v}'_T + \rho\sigma\frac{x_T}{\hat{w}_T}e^{\kappa' T}\left(\frac{v_0 - \theta}{\kappa' - \kappa}\left(e^{(\kappa' - \kappa)T} - 1\right) + \frac{\theta}{\kappa'}\left(e^{\kappa' T} - 1\right)\right). \tag{4.15}$$

An implementation of this formula is given in [16]. As examples we provide a table and a figure. Note that all of the values for ρ parameter listed in Table 4.1 are very close to 1 or -1 except for two dates: 02.03 and 16.03. Table 4.2 lists the local volatilities Equation 4.15 as well as the implied volatility for a call option with strike $K = 95$ and maturity 29.04 for the rest of the dates using the approximation Equation 4.15. Our main observation on this table is that the local and implied volatilities seem relatively close to each other.

Figure 4.3 gives the entire local volatilty surfaces using the same technique for the days 01.03, 15.03. The surface on top is for the day 15.03 and the one below is for 01.03. We observe that their shapes seem similar and smooth, but as already indicated, the volatility for 15.03 is uniformly greater than that of 01.03.

Table 4.2: Local Volatility vs. Heston Implied Volatility K=95,Maturity=29.04.2016

	Local Volatility	Heston Implied Volatility
01.03.2016	0.2479	0.2538
03.03.2016	0.2038	0.2446
04.03.2016	0.2376	0.2436
07.03.2016	0.2468	0.2531
08.03.2016	0.2309	0.2494
09.03.2016	0.2264	0.2265
10.03.2016	0.2343	0.2236
11.03.2016	0.2130	0.2070
14.03.2016	0.2204	0.1911
15.03.2016	0.1760	0.2217
17.03.2016	0.1760	0.1811
18.03.2016	0.2062	0.1519
21.03.2016	0.2186	0.1663
22.03.2016	0.2356	0.2280
23.03.2016	0.2490	0.2454
24.03.2016	0.2502	0.2349
25.03.2016	0.2593	0.2562
28.03.2016	0.2515	0.2383
29.03.2016	0.2426	0.2131
30.03.2016	0.2418	0.2054
31.03.2016	0.2211	0.1785

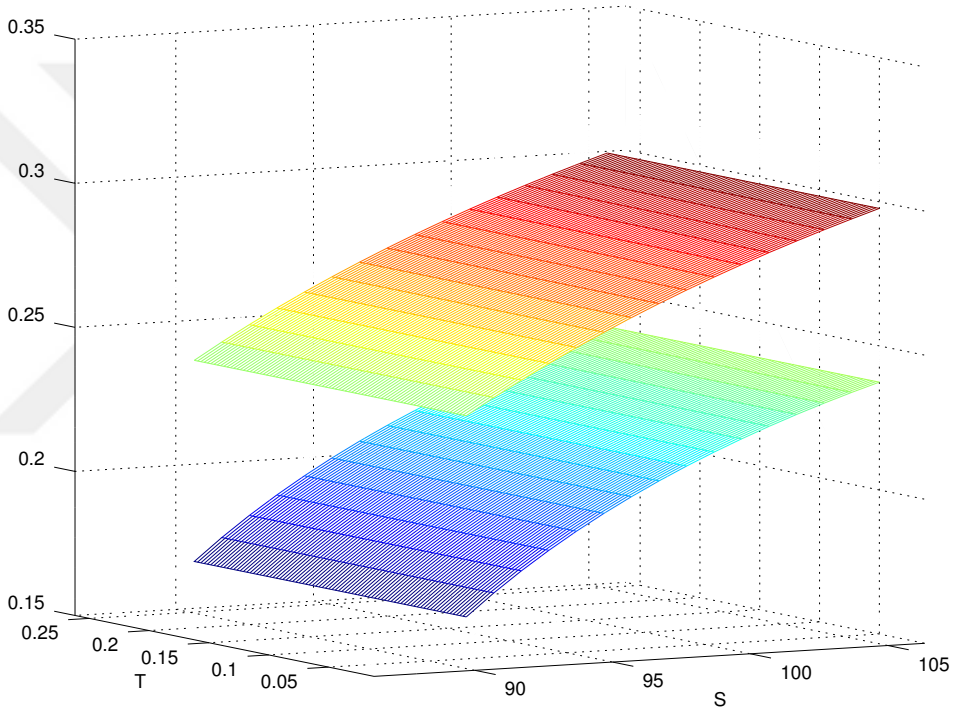

Figure 4.3: Local Volatility Surfaces for 01.03.2016 and 15.03.2016

CHAPTER 5

Conclusion

In this chapter, we comment further on our results and suggest several directions for future research.

In Chapter 3, we saw that model prices computed using historical estimation of the local volatility function give prices below market prices. Results of Section 3.2.3 suggest that hedging with these model prices lead to great hedging errors. When we use market prices for hedging we get better hedging results as seen in graphics of Section 3.2.5; but the results are almost the same as those obtained from simple Black scholes. In the last chapter we have looked at several hedging examples using the local volatility model implied by the Heston model fitted to market price data. Our main observation in these examples are two: the absolute value of the hedging error doesn't change significantly from that of BS but it leads to different hedge error processes (this is in contrast to results in Chapter 3).

For future work, the following goals seem relevant: doing historical fits of local volatility function allowing dependence on time, testing the fit-hedge-price calculations on more extensive data (more time periods, more strikes and maturities) and running the hedging algorithm on options not traded in the market.

REFERENCES

[1] F. Black and M. Scholes, The pricing of options and corporate liabilities, The journal of political economy, pp. 637–654, 1973.

[2] T. F. Coleman, Y. Li, and A. Verma, Reconstructing the unknown local volatility function, in *Quantitative analysis in financial markets: collected papers of the New York University Mathematical Finance Seminar*, volume 2, p. 192, 2001.

[3] J. C. Cox, J. E. Ingersoll Jr, and S. A. Ross, A theory of the term structure of interest rates, Econometrica: Journal of the Econometric Society, pp. 385–407, 1985.

[4] E. Derman and I. Kani, Riding on a smile, Risk, 7(2), pp. 32–39, 1994.

[5] B. Dupire et al., Pricing with a smile, Risk, 7(1), pp. 18–20, 1994.

[6] A. Friedman, *Partial differential equations of parabolic type*, Dover, 2013.

[7] J. Gatheral, *The volatility surface: a practitioner's guide*, volume 357, John Wiley & Sons, 2011.

[8] J. Geng, Calibration of local volatility models and proper orthogonal decomposition reduced order modeling for stochastic volatility models, 2016.

[9] S. L. Heston, A closed-form solution for options with stochastic volatility with applications to bond and currency options, Review of financial studies, 6(2), pp. 327–343, 1993.

[10] R. Kamp, Local volatility modelling, 2009.

[11] I. Karatzas and S. Shreve, *Brownian motion and stochastic calculus, second edition*, volume 113, Springer Science & Business Media, 1991.

[12] H. Kushner and P. G. Dupuis, *Numerical methods for stochastic control problems in continuous time*, volume 24, Springer Science & Business Media, 2013.

[13] D. Lamberton and B. Lapeyre, *Introduction to stochastic calculus applied to finance, second edition*, Chapman and Hall / CRC press, 2008.

[14] O. M. Mert, Applications of the heston model on bist30 warrants: hedging and pricing, master's thesis, 2016.

[15] R. C. Merton, Theory of rational option pricing, The Bell Journal of economics and management science, pp. 141–183, 1973.

[16] F. D. Rouah, *The Heston Model and its Extensions in Matlab and C*, John Wiley & Sons, 2013.